Industrial Batch-type Tube ALD Reactor Enables TiO_2 and Al-doped TiO_2 Deposition on Large-scale Solar Silicon Wafers by TDMAT and H_2O

Xinyuan Wu[1], Borong Sang[1], Baochen Liao[2], Bram Hoex[1]

[1]*School of Photovoltaic and Renewable Energy Engineering, University of New South Wales, Kensington, Australia*
[2]*School of Information Science and Technology, Nantong University, Nantong, Jiangsu, ChinaIntroduction*

Titanium oxide (TiO_2) is widely used as a versatile material in photovoltaic devices. It has extraordinary optical properties, such as relatively low parasitic absorption and high refractive index[1,2]. Furthermore, the excellent c-Si surface passivation properties of this layer was also reported in the last decade. TiO_2 films grown by low-temperature thermal atomic layer deposition (ALD) using titanium tetrachloride ($TiCl_4$) and H_2O as the precursors, can reduce the effective surface recombination rate to 8.3 cm/s on p-type float-zone c-Si wafers[3,4]. In addition, TiO_2 can be used as an electron selective contact as it has a low conduction band offset and a significant valence band offset. and contributes to 23.1% silicon solar cell efficiency[5]. In recent years, TiO_2 has also been used in perovskite solar cells[6]. However, TiO_2 easily crystallises, resulting in a loss in c-Si surface passivation, after annealing[7]. Al doping can enhance the thermal stability of TiO_2, making it more compatible with the silicon solar cells' process window. $TiCl_4$ is the dominant precursor for the ALD TiO_2 process, but severe Cl contamination, low reactivity, and corrosive by-products (e.g., HCl) constrain the ALD TiO_2 application in the industry. Tetrakis(dimethylamido)titanium (TDMAT) is a metal-organic precursor is an appealing candidate to replace $TiCl_4$ for the ALD process as it has a high reactivity and does not produce corrosive by-products. In this work, we developed the thermal ALD TiO_2 process by TDMAT and H_2O in an industrial-scale ALD reactor. The Al-doped TiO_2 process was investigated as well.

Experiments

For growth rate optimisation, 8-inch p-type double-side polished Cz-Si wafers (Orientation: <100>, ~725 um, ~0.005 Ω·cm) were cut into 156 cm × 156 cm, and then RCA (Radio Corporation of America) cleaned. Native SiO_2 was removed by ~1% HF dip.The ALD processes were conducted in a Leadmicro QL200 ALD reactor. This reactor can deposit 200 wafers in one time. For TiO_2 deposition, TDMAT and H_2O were used as the precursors, and N_2 was the purge gas. The TDMAT canister was heated up to 80 °C, and related pipes were heated to 150 °C to avoid downstream condensation. The water pipes were heated up to 95 °C. The set-temperature of the reaction chamber was 120 °C. It was noted that, before the process, the TDMAT canister and precursors' pipes were heated from room temperature for above one hour to achieve uniform inner temperature status. After wafer loading, the chamber was pumped down to 0.39 mbar and heated to 120 °C. The chamber preheating continued for 15~20 minutes to stabilise heating units and avoid overheating.
After deposition, we chose 9 points per wafer to measure the TiO_2 thickness and extract the optical properties using a JA Woollam M-2000 DI ellipsometer. The imaginairy part of the dielectric function was fitted by the Tauc-Lorentz model. The uniformity was calculated by the equation below:

$$Thickness\ uniformity\ (\%) = \frac{Maximun\ thickness - \ Minimum\ thickness}{2 \times Average\ thickness} \times 100\%$$

For lifetime samples, *p*-type double-side etched Cz-Si wafers (Orientation: <100>, ~170 um, 1.4~1.6 Ω·cm) were RCA cleaned and treated with ~1% HF dip to remove native SiO_2. 150 cycles (around 10 nm) of TiO_2 was deposited on both sides of the wafers. Subsequently, the samples underwent a rapid thermal process (RTP) in a MPT Corp. 600XP annealer at a temperature range of 150 to 300 °C at an N_2 atmosphere. For each temperature setting, the stable temperature duration was 10 minutes. The passivation quality of the TiO_2 film was quantified by measuring the effective minority charge carrier lifetime (τ_{eff}) of the symmetrically passivated structures by contactless photoconductance decay (PCD, WCT-120, Sinton Instruments). The implied open-circuit voltage (iV_{oc}) of the samples was extracted according to the method published by Sinton and Cuevas[8,9].The samples for Al-doped

TiO_2 were prepared by the same methods as TiO_2. The ALD cycle ratio of Ti to Al was 5:1. 25 super-cycles (150 cycles in total) were processed for the thickness and lifetime samples.

Results and discussion

Table 1 shows the thickness measurement results of 150-cycle deposition of optimised TiO_2 and Al-doped TiO_2 processes. The with-in wafer uniformities for TiO_2 and Al-doped TiO_2 are 6.47% and 2.22%, respectively. Furthermore, the Al-doped TiO_2 was found to be thicker and more uniform as Al_2O_3 has a higher growth rate, and TMA is easy to nucleate[10-13]. Table 2 summarises the wafer-to-wafer uniformity of the chamber in a one-run process, and the corresponding value is 1.92%. This indicates that the wafers were uniformly exposed to the precursor atmosphere, and the reaction was self-limiting for all wafers..

Table 1 Thickness mapping of optimised TiO_2 and doped-TiO_2 process.

Measurement point	TiO_2 Thickness (nm)	Al-doped TiO_2 Thickness (nm)
Point 1	9.69	14.61
Point 2	10.20	14.44
Point 3	10.07	14.79
Point 4	9.11	14.25
Point 5	8.97	14.15
Point 6	9.16	14.23
Point 7	9.34	14.21
Point 8	9.20	14.50
Point 9	9.77	14.27
Average	9.50	14.38
With-in wafer uniformity	6.47%	2.22%

Table 2 Average TiO_2 thickness of each position wafer in the ALD reactor chamber.

Wafer position in the chamber	Average thickness (nm)
bottom corner	9.51
bottom mid	9.28
top corner	9.48
top mid	9.15
Wafer-to-wafer uniformity	1.92%

The growth rate per cycle (GPC) was estimated from conducting depositions with a different number of ALD cycles. Figure 1 shows the TiO_2 thickness as a functi of the number of ALD cycles. The GPC was found to be around 0.085 nm/cycle. This growth rate is consistent with Xie et al.'s results[11] and faster than using $TiCl_4$ as precursor[14]. The refractive index for the intrinsic TiO_2 films was in the range reported by Sarkar et al.[15] and Siefke et al.[16]. The refractive index of Al-doped TiO_2 was found to be lower but still uniformly distributed in a single wafer. This is because the refractive index of Al_2O_3 is ~1.7 at 632.8 nm wavelength.

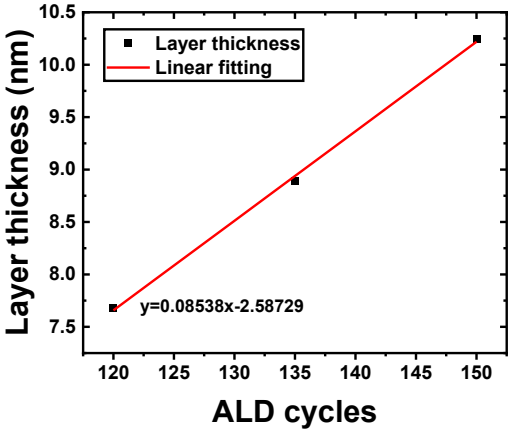

Figure 1. Intrinsic TiO_2 thickness as a function of ALD cycles.

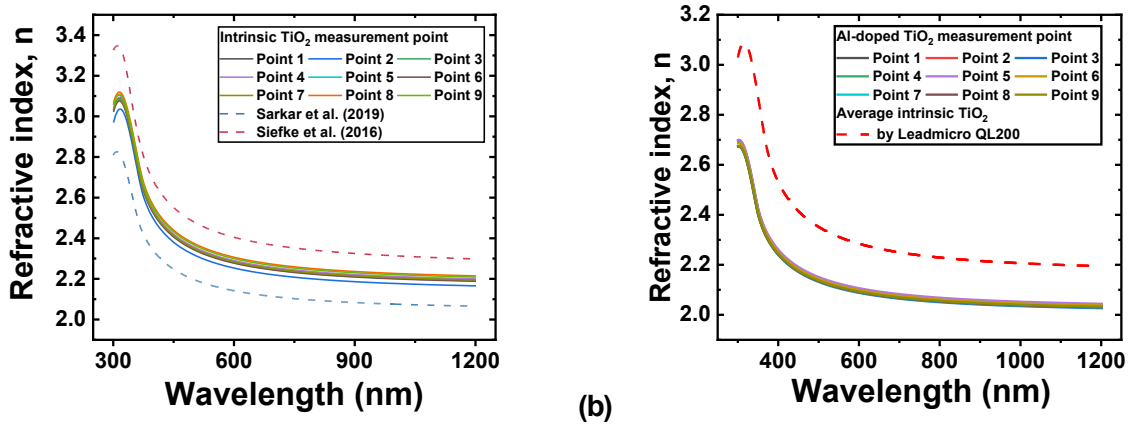

Figure 2. Refractive index as a function of wavelengths measured different points in a wafer of (a) intrinsic TiO_2 layer (this work) and compared with TiO_2 optical models measured by Sarkar et al.15 and Siefke et al.16 (b) Al-doped TiO2 layer and compared with average values of Figure 2. (a).

Figure 3 shows the measured τ_{eff} and the corresponding iV_{oc} for the symmetrically deposited TiO_2 on undiffused p-type silicon samples after RTP annealing. The best average τ_{eff} was achieved after 250 °C annealing with a value of 134 µs. Moreover, the corresponding average iV_{oc} was found to be 0.64 V. We could observe a significant drop when the annealing temperature was 300 °C. This could be attributed to the crystallisation of TiO_2[3,14].

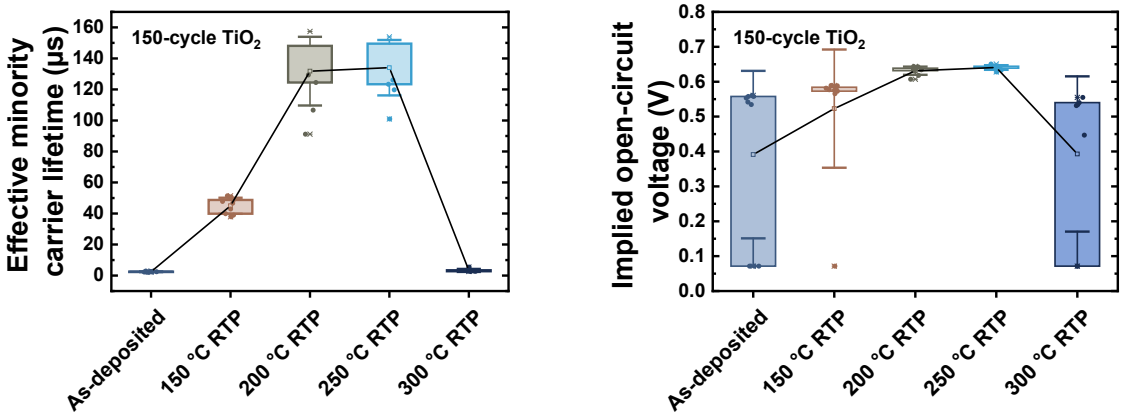

Figure 3. (a) Measured effective minority carrier lifetimes and (b) corresponding implied V_{oc} values of symmetrical intrinsic TiO_2 deposited undiffused double-side etched p-type silicon wafers as a function of the annealing status.

Figure 4 shows the effective minority carrier lifetime for Al-doped TiO_2. When the TiO_2 was doped with Al, the best passivation was achieved after annealing at 200 °C with an average lifetime of 260 µs and a 0.67 V iV_{oc}. These results were significantly better than intrinsic TiO_2. It is worth noting that the average iV_{oc} value was still 0.64 V after 300 °C RTP annealing. This proves that Al doping enhanced both the level of surface passivation as well as the thermal stability of the TiO_2 layers.

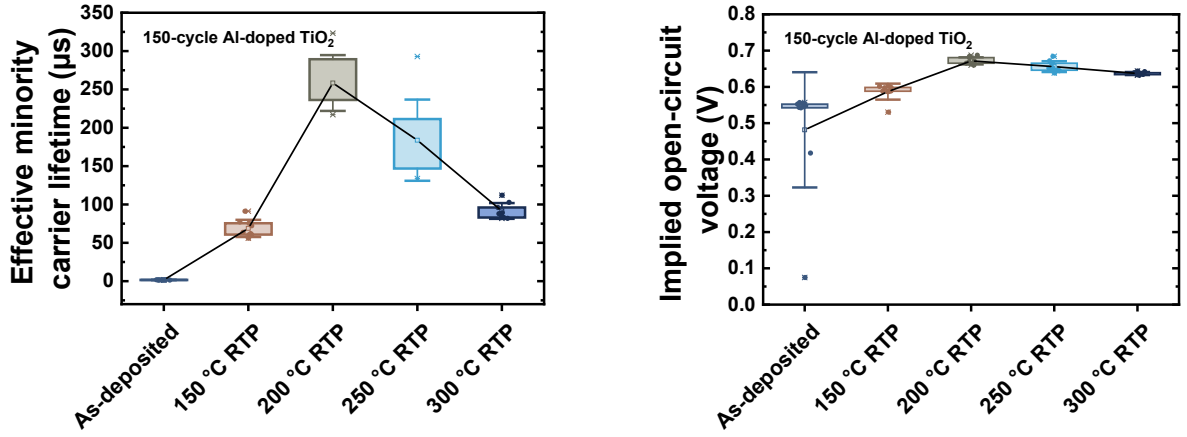

(a) (b)

Figure 4. (a) Measured effective minority carrier lifetimes and (b) corresponding implied V_{oc} values of symmetrical Al-doped TiO_2 deposited undiffused double-side etched p-type silicon wafers as a function of the annealing status.

Conclusion

In summary, we successfully enabled the thermal ALD TiO_2 process by TDMAT and H_2O in a large-volume industrial ALD reactor. The optimised with-in wafer and wafer-to-wafer uniformities were found to be 6.47% and 1.92%, respectively. The best level of surface passivaiton was achieved after 250 °C RTP annealing temperature with a 134 µs τ_{eff} and 0.64 V iV_{oc} on 1.4~1.6 Ω·cm p-type silicon wafers. In addition, Al-doping effectively improve the with-in wafer uniformity, the level of surface passivaiton and high-temperature tolerance. Future work will focus on element analysis and TiO_2/Al-doped TiO_2 application in photovoltaic devices.

References

1 Szindler, M., Szindler, M. M., Boryło, P. & Jung, T. Structure and optical properties of TiO₂ thin films deposited by ALD method. *Open Physics* **15**, 1067-1071 (2017). https://doi.org:10.1515/phys-2017-0137

2 Tang, H., Prasad, K., Sanjinès, R., Schmid, P. E. & Lévy, F. Electrical and optical properties of TiO₂anatase thin films. *Journal of Applied Physics* **75**, 2042-2047 (1994). https://doi.org:10.1063/1.356306

3 Liao, B., Hoex, B., Shetty, K. D., Basu, P. K. & Bhatia, C. S. Passivation of Boron-Doped Industrial Silicon Emitters by Thermal Atomic Layer Deposited Titanium Oxide. *IEEE Journal of Photovoltaics* **5**, 1062-1066 (2015). https://doi.org:10.1109/jphotov.2015.2434596

4 Liao, B., Hoex, B., Aberle, A. G., Chi, D. & Bhatia, C. S. Excellent c-Si surface passivation by low-temperature atomic layer deposited titanium oxide. *Applied Physics Letters* **104**, 253903 (2014). https://doi.org:10.1063/1.4885096

5 Bullock, J. *et al.* Dopant‐Free Partial Rear Contacts Enabling 23% Silicon Solar Cells. *Advanced Energy Materials* **9**, 1803367 (2019). https://doi.org:10.1002/aenm.201803367

6 Seo, J.-Y. *et al.* Boosting the Efficiency of Perovskite Solar Cells with CsBr-Modified Mesoporous TiO₂Beads as Electron-Selective Contact. *Advanced Functional Materials* **28**, 1705763 (2018). https://doi.org:10.1002/adfm.201705763

7 Liu, Y. *et al.* A novel passivating electron contact for high-performance silicon solar cells by ALD Al-doped TiO2. *Solar Energy* **228**, 531-539 (2021). https://doi.org:10.1016/j.solener.2021.09.083

8 Sinton, R. A. & Cuevas, A. Contactless determination of current‐voltage characteristics and minority ‐ carrier lifetimes in semiconductors from quasi ‐ steady ‐ state photoconductance data. *Applied Physics Letters* **69**, 2510-2512 (1996). https://doi.org:10.1063/1.117723

9 Sinton, R. A., Cuevas, A. & Stuckings, M. in *Conference Record of the Twenty Fifth IEEE Photovoltaic Specialists Conference-1996.* 457-460 (IEEE).

10 Dingemans, G., Seguin, R., Engelhart, P., Sanden, M. C. M. V. D. & Kessels, W. M. M. Silicon surface passivation by ultrathin Al2O3films synthesized by thermal and plasma atomic layer deposition. *physica status solidi (RRL) - Rapid Research Letters* **4**, 10-12 (2010). https://doi.org:10.1002/pssr.200903334

11 Xie, Q. *et al.* Atomic layer deposition of TiO2 from tetrakis-dimethyl-amido titanium or Ti isopropoxide precursors and H2O. *Journal of Applied Physics* **102**, 083521 (2007). https://doi.org:10.1063/1.2798384

12 Simonsen, M. E. & Søgaard, E. G. Identification of Ti Clusters during Nucleation and Growth of Sol—Gel-Derived TiO₂ Nanoparticles. *European Journal of Mass Spectrometry* **19**, 265-273 (2013). https://doi.org:10.1255/ejms.1232

13 Bulusu, A. *et al.* The Mechanical Behavior of ALD-Polymer Hybrid Films Under Tensile Strain. *Advanced Engineering Materials* **17**, 1057-1067 (2015). https://doi.org:10.1002/adem.201400431

14 Liao, B. *et al.* A Comprehensive Fundamental Understanding of Atomic Layer Deposited Titanium Oxide Films for c-Si Solar Cell Applications. *IEEE Journal of Photovoltaics* **11**, 319-328 (2021). https://doi.org:10.1109/jphotov.2021.3050264

15 Sarkar, S. *et al.* Hybridized Guided-Mode Resonances via Colloidal Plasmonic Self-Assembled Grating. *ACS Applied Materials & Interfaces* **11**, 13752-13760 (2019). https://doi.org:10.1021/acsami.8b20535

16 Siefke, T. *et al.* Materials Pushing the Application Limits of Wire Grid Polarizers further into the Deep Ultraviolet Spectral Range. *Advanced Optical Materials* **4**, 1780-1786 (2016). https://doi.org:10.1002/adom.201600250